New Phytologist

Exploring the role of biotic factors in regulating the spatial variability in land surface phenology across four temperate forest sites

Journal:	*New Phytologist*
Manuscript ID	NPH-MS-2023-44693
Manuscript Type:	Full Paper
Date Submitted by the Author:	30-Aug-2023
Key Words:	plant phenology, land surface phenology, intra-site variability, plant functional types, plant functional traits, biotic controls, NEON

Complete List of Authors:
Zhao, Yingyi; The University of Hong Kong, School of Biological Sciences
Wang, Zhihui; Guangzhou Institute of Geography Guangdong Academy of Sciences, Guangdong Provincial Key Laboratory of Remote Sensing and Geographical Information System, Guangdong Open Laboratory of Geospatial Information Technology and Application
Yan, Zhengbing; Institute of Botany Chinese Academy of Sciences, State Key Laboratory of Vegetation and Environmental Change
Moon, Minkyu; Boston University, Department of Earth and Environment; Kangwon National University, School of Natural Resources and Environmental Science
Yang, Dedi; Brookhaven National Laboratory, Environmental and Climate Sciences Department
Meng, Lin; Vanderbilt University, Earth and Environmental Science
Bucher, Solveig Franziska; Friedrich Schiller University Jena, Institute of Ecology and Evolution
Wang, Jing; SYSU, Biological science
Song, Guangqin; The University of Hong Kong, School of Biological Sciences
Guo, Zhengfei; The University of Hong Kong, School of Biological Sciences
Su, Yanjun; Institute of Botany, Chinese Academy of Sciences, State Key Laboratory of Vegetation and Environmental Change
Wu, Jin; University of Hong Kong, School of Biological Sciences

SCHOLARONE™
Manuscripts

Title: Exploring the role of biotic factors in regulating the spatial variability in land surface phenology across four temperate forest sites

Author List: Yingyi Zhao[1], Zhihui Wang[2], Zhengbing Yan[3], Minkyu Moon[4,5], Dedi Yang[6], Lin Meng[7], Solveig Franziska Bucher[8,9], Jing Wang[10], Guangqin Song[1], Zhengfei Guo[1], Yanjun Su[11], Jin Wu[1,12]*

Author Affiliations:

(1) School of Biological Sciences, The University of Hong Kong, Pokfulam, Hong Kong, China

(2) Guangdong Provincial Key Laboratory of Remote Sensing and Geographical Information System, Guangdong Open Laboratory of Geospatial Information Technology and Application, Guangzhou Institute of Geography, Guangdong Academy of Sciences, Guangzhou 510070, China

(3) State Key Laboratory of Vegetation and Environmental Change, Institute of Botany, Chinese Academy of Sciences, Xiangshan, Beijing, China

(4) Department of Earth and Environment, Boston University, Boston, MA 02215, USA

(5) School of Natural Resources and Environmental Science, Kangwon National University, Chuncheon 24341, Korea

(6) Environmental and Climate Sciences Department, Brookhaven National Laboratory, Upton, NY 11973, USA

(7) Department of Earth and Environmental Sciences, Vanderbilt University, Nashville, TN, USA

(8) Institute of Ecology and Evolution with Herbarium Haussknecht and Botanical Garden, Department of Plant Biodiversity, Friedrich Schiller University Jena, D-07743 Jena, Germany

(9) German Centre for Integrative Biodiversity Research (iDiv) Halle-Jena-Leipzig, D-04103 Leipzig, Germany

(10) School of Ecology, Shenzhen Campus of Sun Yat-sen University, Shenzhen, Guangdong, China

(11) State Key Laboratory of Vegetation and Environmental Change, Institute of Botany, Chinese Academy of Sciences, Beijing 100093, China

(12) Institute for Climate and Carbon Neutrality, The University of Hong Kong, Pokfulam, Hong Kong, China

For Peer Review

*** Corresponding Author:** Jin Wu

School of Biological Sciences, The University of Hong Kong, Pokfulam Road, Hong Kong Special Administrative Region, China (email: jinwu@hku.hk; phone: +852 2299-0655)

Figures/Tables Record:

Number of figures/tables: 6 figures, 3 tables

Supporting materials: 9 figures, 3 tables

Word count: 6491

For Peer Review

Summary (200 words limit)

- Land surface phenology (LSP), the characterization of plant phenology with satellite data, is essential for understanding the effects of climate change on ecosystem functions. Although ecosystem-scale LSP variability has been linked to climate, considerable LSP variation persists within local landscapes, and the role of biotic factors in regulating such variation remain underexplored.
- In this study, we selected four NEON terrestrial sites with minor topographic relief to investigate how biotic factors regulate intra-site LSP variability. We utilized plant functional type (PFT) maps, functional traits, and LSP data to assess the explanatory power of biotic factors for the start and end of season (SOS and EOS) variability.
- Our results indicate that PFTs alone explain only 0.8% to 23.4% of intra-site SOS and EOS variation, whereas including functional traits significantly improves explanatory power, with cross-validation correlations ranging from 0.50 to 0.85. Functional traits related to competitive ability and productivity (e.g., canopy height, plant area index, and leaf mass per area) were important variables, although their relative contributions varied across sites.
- These findings demonstrate that biotic factors are significant for regulating intra-site LSP variability, and plants adopt diverse strategies to cope with the environment, which ultimately determine various ecological processes.

Key words: Plant phenology, land surface phenology, intra-site variability, plant functional types, plant functional traits, biotic controls, NEON

For Peer Review

1. Introduction

Plant phenology, the study of recurring biological events in plant organisms, is essential for understanding various ecosystem processes, such as land-atmosphere interactions, and species competition and coexistence (Cleland *et al.*, 2007; Forrest & Miller-Rushing, 2010; Wolkovich *et al.*, 2014). Many studies have demonstrated that plant phenology is sensitive to various climatic factors, such as temperature and photoperiod (Polgar & Primack, 2011; Li *et al.*, 2019; Moon *et al.*, 2021b). Phenological patterns observed over large spatial scales are closely aligned with climatic variation along elevational and latitudinal gradients (Dragoni & Rahman, 2012; Shen *et al.*, 2022). However, significant inter- and intra-specific phenological variation has also been observed at local scales (Cole & Sheldon, 2017; Wu *et al.*, 2021; Zhao *et al.*, 2022), with evidence suggesting that factors beyond climate may regulate phenology.

In recent decades, there has been a growing interest in examining the spatial and temporal variability of phenology within forest landscapes and their roles in determining ecosystem processes and forest ecosystem responses to climate change (Cleland *et al.*, 2007; Pau *et al.*, 2011; Xia *et al.*, 2015). To support such research, extensive phenology data are available, including field-based, proximate remote sensing (e.g., PhenoCams), and satellite observations. Field-based observations provide precise species-specific phenology data but are often limited to a small number of species and regions due to substantial labor and time costs (Zeng *et al.*, 2020; Wu *et al.*, 2021). Proximate remote sensing methods are more cost-effective and can effectively capture individual- to ecosystem-scale phenology but remain restricted to a narrow set of trees or species due to the limited field of view (Xie *et al.*, 2018; Delpierre *et al.*, 2020). Satellite remote sensing overcomes the spatial constraint by providing measurements over vast areas with frequent acquisitions, enabling timely monitoring of vegetation dynamics. Referred to as land surface phenology (LSP), satellite-detected vegetation phenology has been extensively used to study phenological trends and variability with climate change over large geographical areas (Garonna *et al.*, 2014; Melaas *et al.*, 2016; Shen *et al.*, 2022).

The increasing availability of abundant phenology data and other auxiliary data has significantly advanced investigations into drivers of local-scale phenological variation. Within forest landscapes, several studies have identified forest stand characteristics and plant functional types (PFTs) as potential explanatory variables for spatial variation in LSP (Hwang *et al.*, 2011; Misra *et al.*, 2018; Wang *et al.*, 2021). Moreover, evidence from both field and remote sensing observations suggests that variations in functional traits are associated with

For Peer Review

phenological variation (Osada, 2017; Yin *et al.*, 2018; Adams *et al.*, 2021). For example, traits related to competitive ability, such as plant height (or canopy height) and specific leaf area, have been suggested to be linked to phenology (Sun *et al.*, 2006; Liu *et al.*, 2021; Sporbert *et al.*, 2022). Also, traits related to water use efficiency and resistance to disturbance are associated with the timing of various phenological stages (Bucher *et al.*, 2019; Bucher & Römermann, 2021). These studies imply that biotic factors may play a crucial role in regulating local-scale phenological variability. However, most of these studies have been constrained to limited sites and data, resulting in a lack of comprehensive research on the association between biotic factors and vegetation phenology. Additionally, previous studies might misinterpret the roles of biotic factors in regulating intra-site phenological variability since significant within-site environmental variation is not explicitly considered.

Recently, a variety of remote sensing techniques have emerged as effective tools for deriving multiple functional traits across different spatial scales. Among these, airborne imaging spectroscopy has been proven particularly effective in measuring an array of plant functional traits at the fine scale over large spatial areas due to its high spatial and spectral resolutions (Dahlin *et al.*, 2013; Wang *et al.*, 2019; Liu *et al.*, 2023). This technique relies on the strong association between leaf/canopy reflectance spectra and plant morphological, biochemical, and physiological properties, and it has been extensively employed to map foliar functional traits, such as leaf mass per area (LMA), chlorophyll content, and nitrogen content, with high accuracy (Martin *et al.*, 2008; Asner *et al.*, 2015; Wang *et al.*, 2020). In addition to foliar traits, traits associated with plant structural properties have also gained significant interest, as they are linked to a variety of ecosystem functions like plant growth, resilience to disturbance, and nutrient fluxes (Van Ewijk *et al.*, 2014; Larue *et al.*, 2019; Maeda *et al.*, 2022). Light Detection and Ranging (LiDAR) characterizes plant structural properties by offering three-dimensional data on vegetation features and canopy elements, which has been used to derive a number of structural traits, such as canopy height, plant area index (PAI), and height entropy (LaRue *et al.*, 2020; Guillén-Escribà *et al.*, 2021; Hakkenberg & Goetz, 2021). The establishment of the National Ecological Observatory Network (NEON), a large-scale ecological observatory, now makes airborne imaging spectroscopy and LiDAR data across representative ecosystems in the United States available, enabling researchers to generate both foliar and structural traits over large spatial coverages across multiple ecosystems. This, together with the increasing availability of LSP data over forest landscapes, presents timely opportunities to investigate the biotic regulation of intra-site phenological variability.

For Peer Review

The goal of this study is to assess the role of biotic factors in regulating intra-site phenological variability. We selected four NEON terrestrial sites with minor topographic relief to retain relatively homogeneous climatic conditions within each site and minimize the intra-site climate impact. We used multi-year LSP data derived from the Harmonized Landsat 8 and Sentinel-2 (HLS) data (Bolton *et al.*, 2020), plant functional traits derived from airborne imaging spectroscopy (Wang *et al.*, 2020) and LiDAR data, and satellite-derived PFT maps to assess the influence of biotic factors on LSP variation. Specifically, we addressed the following questions: (1) To what extent do PFTs contribute to the total phenological variability in landscapes with multiple PFTs? (2) To what extent can plant functional traits explain the intra-site phenological variability, and which functional traits are important for explaining phenological variation? (3) What potential ecological strategies do plants employ to regulate intra-site phenological variability? By answering these questions, we aim to enhance our understanding of biotic influences on phenological variation and the mechanisms underlying this variation.

2. Materials and Methods

2.1. Study sites

Four terrestrial sites from NEON with minor topographic relief were selected for this study (Fig. 1, Table 1). These sites include Dead Lake (DELA), Smithsonian Environmental Research Center (SERC), Treehaven (TREE), and University of Notre Dame Environmental Research Center (UNDE). Spanning three distinct ecoclimatic domains, these sites have mean annual temperatures ranging from 4.3 to 17.6 °C and mean annual precipitation ranging from 797 to 1370 mm yr^{-1}. To ensure a relatively homogeneous environment, we defined an 8 km × 8 km study area for each site, characterized by an elevation range below 100 m. This approach helped minimize the impact of climate variation on intra-site phenological variation. All these sites are dominated by deciduous forests, mixed forests, or woody wetlands with a diverse array of tree species present (Table 1). Furthermore, sufficient biotic data (i.e., information on plant functional types and functional traits) and phenology data are available at these sites, enabling the investigation of the role of biotic factors in explaining intra-site phenological variation.

For Peer Review

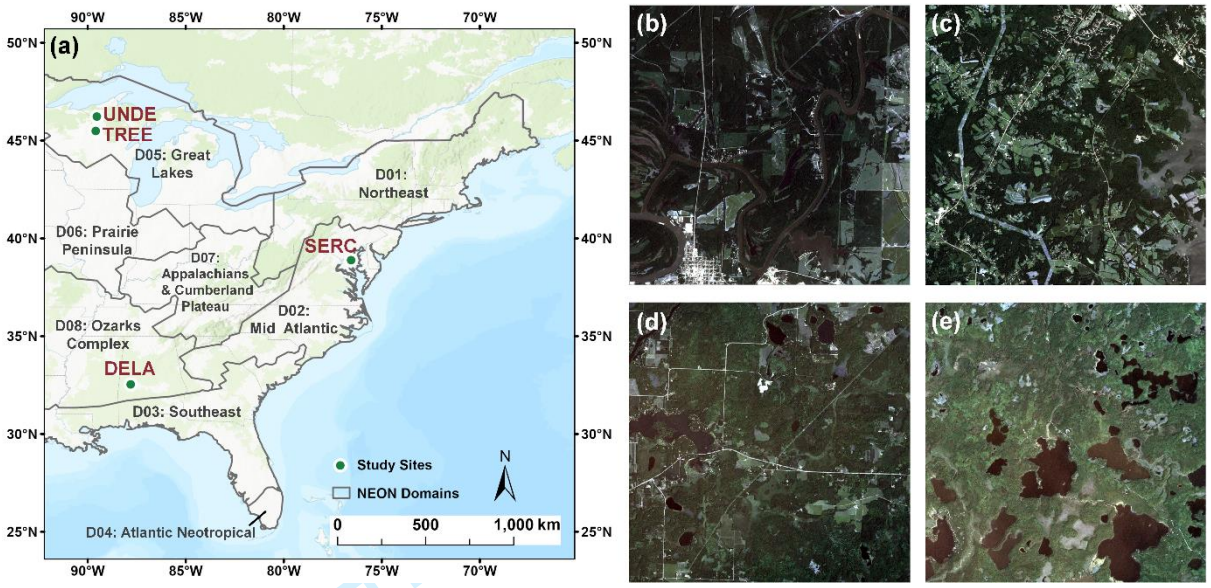

Fig. 1. Study sites and true color images from PlanetScope. (a) Locations of the four study sites (green dots) over three NEON domains; and true color images (8 km × 8 km) of the study area at each site: (b) DELA; (c) SERC; (d) TREE; (e) UNDE.

Table 1. Location, climate, the range of elevation, ecoclimate domain, and dominant tree species of each study site.

Site	Location	Mean annual temperature (°C)	Mean annual precipitation (mm yr^{-1})	Range of elevation (m)	Ecoclimate domain	Dominant tree species
DELA	32.542°N, 87.804°W	17.6	1370	17-54	08	*Quercus nigra* L., *Celtis laevigata* Willd., *Nyssa sylvatica*, *Carya ovata*, *Fraxinus pennsylvanica*
SERC	38.893°N, 76.560°W	13.6	1075	0-74	02	*Liriodendron tulipifera, Fagus grandifolia, Liquidambar styraciflua*

For Peer Review

TREE	45.492°N, 89.594°W	4.8	797	439-526	05	*Acer saccharum, Acer rubrum, Abies balsamea, Alnus incana*
UNDE	46.232°N, 89.542°W	4.3	802	494-593	05	*Acer rubrum, Acer saccharum, Populus tremuloides, Betula papyrifera*

*Note: DELA-Dead Lake; SERC-Smithsonian Environmental Research Center; TREE-Treehaven; UNDE-University of Notre Dame Environmental Research Center. Ecoclimate domain: 02-Mid Atlantic; 05-Great Lakes; 08-Ozarks Complex.

2.2. Materials

2.2.1 LSP data

In this study, we utilized the 30-m spatial resolution LSP data derived from time-series HLS data collected between 2016 and 2021. For LSP data from 2016 to 2019, we used the Multi-Source Land Surface Phenology (MSLSP) product which is available at the NASA Land Processes Distributed Active Archive Center (LP DAAC). This product estimates the transition dates of key phenophases—such as the start of greenup, mid-greenup, maturity, the start of greendown, mid-greendown and dormancy—at a 30 m spatial resolution using a time series of two-band Enhanced Vegetation Index (EVI2) from HLS data (Bolton *et al.*, 2020). These phenological metrics are highly consistent with those derived from MODIS and, in most ecosystems, display strong agreement with phenocam-derived phenological metrics. In this study, we considered the 'mid-greenup' and 'mid-greendown' metrics as the start (SOS) and end of growing season (EOS), respectively. These metrics are defined as the timing when the EVI2 time series cross 50% of the EVI2 amplitude during the greenup and greendown periods. Comparisons of HLS-derived SOS and EOS against local-scale phenology measurements and a phenology product with a 3 m spatial resolution demonstrate the high quality and significant details of HLS-derived phenological metrics (Moon *et al.*, 2021a). For LSP data from 2020 to 2021, we employed the same method used for generating the MSLSP product to obtain the phenological metrics with HLS data.

2.2.2 Foliar functional trait data

For Peer Review

For each study site, maps depicting various foliar functional traits are available at https://tinyurl.com/neontraits1, as generated by Wang *et al.* (2020). These trait maps were created by developing trait models that integrated field trait measurements and airborne hyperspectral imagery collected in 2017. The hyperspectral imagery was acquired using an imaging spectrometer mounted on the NEON Airborne Observation Platform (AOP), which measures 426 bands between 380 and 2500 nm with a 1 m spatial resolution. The NEON AOP typically conducts site-specific flight surveys from March to October to capture hyperspectral imagery in the peak growing season at each site. In total, maps of 26 foliar functional traits and their associated uncertainties are provided for our four study sites. The mapped functional traits include both leaf biochemical traits, such as carbon content and pigment concentrations, and leaf morphological traits, such as leaf mass per area (LMA). Among these traits, we selected seven traits for this study because they are related to some important ecosystem functions and potentially associated with phenology (Table 2). As our study sites are situated in domains D02, D05 and D08 (Fig. 1), and more than 75% of the pixels across the mapped area in these domains exhibit high confidence for all traits (Wang *et al.*, 2020), the selected functional traits are deemed reliable for the subsequent data analysis.

2.2.3 LiDAR data

LiDAR data were acquired using a full waveform LiDAR instrument mounted on the NEON AOP, covering an area of at least 10 km × 10 km for each NEON site and with a minimum density of four LiDAR shots per square meter. The data collection occurred during the peak greenness period, which coincided with the capture of hyperspectral imagery. Raw full waveforms were processed into projected and corrected discrete return LiDAR point cloud products (NEON, 2023) which were used in this study. LiDAR point clouds covering each site's study area were divided into 1 km × 1 km tiles, with specific details, such as coordinates, intensity, and classifications, recorded for each point. During the pre-processing steps, an isolated voxel filter (IVF) was applied to each tile to identify outlier points, which were removed from the point cloud. Following this, digital terrain models (DTM) were created based on the classified ground points, and height-normalized point clouds were generated by subtracting the DTM from the original point clouds. These normalized point clouds were then used to derive structural traits (Table 2).

Table 2. Plant functional traits and the related functions in the plant community.

Trait	Related functions and ecological meaning

For Peer Review

Mean canopy height (m)	Light interception, canopy hydraulic conductivity, productivity, competitive ability, age classes (Larue *et al.*, 2019; Adams *et al.*, 2021; Maeda *et al.*, 2022)
Plant area index (PAI)	Land-atmosphere interactions, productivity, light interception, competitive ability (Toda & Richardson, 2018; Maeda *et al.*, 2022)
Height skew	Light interception, vegetation composition (Hakkenberg, Zhu, Peet, & Song, 2018; Hakkenberg & Goetz., 2021)
Entropy	Habitat complexity, light interception (Hakkenberg & Goetz, 2021; Larue et al., 2019)
Rugosity	Light interception, habitat structure (Hakkenberg & Goetz, 2021; Larue et al., 2019)
Leaf mass per area (LMA, g m^{-2})	Productivity, competitive ability, photosynthetic capacity, growth performance (Wright *et al.*, 2004; Sun *et al.*, 2006; Poorter *et al.*, 2009)
Mass-based leaf carbon content (mg g^{-1})	Structural compounds, performance (Bucher *et al.*, 2018; Sporbert *et al.*, 2022)
Mass-based leaf nitrogen content (mg g^{-1})	Productivity, photosynthetic capacity (Wright *et al.*, 2004; Bucher *et al.*, 2018; Sporbert *et al.*, 2022)
Area-based chlorophyll concentrations (mg g^{-1})	Photosynthetic capacity, productivity (Croft *et al.*, 2015; Noda *et al.*, 2015)
Mass-based leaf phenolics concentration (mg g^{-1})	Plant defence to environmental disturbances (Kokaly & Skidmore, 2015; Wang *et al.*, 2022)
Mass-based leaf starch concentration (mg g^{-1})	Plant responses to environmental stress (Charrier *et al.*, 2015; Wang *et al.*, 2022)
$\delta^{13}C$ (per mil)	Water use efficiency (Dawson *et al.*, 2002; Brum *et al.*, 2023)

2.2.4 Land cover data

We used land cover data from the United States Geological Survey's (USGS) National Land Cover Database (NLCD; Dewitz & USGS, 2021) for the year 2019 to differentiate plant functional types (PFTs). The NLCD product provides spatially explicit and reliable information regarding land cover across the conterminous United States at a 30 m spatial resolution. This product contains 17 land cover classes, of which 12 are distinct vegetation types that generally correspond to different PFTs. In our study areas, the predominant land cover types include "Deciduous Forest", "Evergreen Forest", "Mixed Forest", "Shrub", "Grassland/Herbaceous", "Pasture/Hay", "Cultivated Cropland", "Woody Wetland" and "Herbaceous Wetland". Alongside these vegetation types, some non-vegetation types, such as "Open Water" and "Developed area", are present within the study sites. Since our focus is on the phenology of

For Peer Review

natural vegetation, areas occupied by non-vegetation and cultivated vegetation were excluded from further analysis.

2.2.5 PlanetScope imagery

In this study, we also utilized PlanetScope imagery, operated by Planet Lab Inc., to further eliminate non-vegetated area (San Francisco, CA; Planet, 2022). The orthorectified and radiometrically corrected PlanetScope surface reflectance data (Level 3B) has four bands (bule, green, red, and near-infrared) with a 3 m spatial resolution, which is effective in characterizing land surfaces and allows for more precise differentiation between vegetated and non-vegetated areas. We used the PlanetScope data obtained during the peaking growing season of 2018 for each site and generated NDVI data from the raw PlanetScope data. By setting an NDVI value threshold (i.e., 0.65), the NDVI data facilitated the removal of non-vegetated areas by filtering out non-vegetated pixels.

2.3. Methods

2.3.1 Pre-processing LSP data and foliar functional trait data

For each site, we extracted the maps of SOS and EOS from the LSP data of each year from 2016 to 2021 individually. Subsequently, we clipped these phenology maps to the defined 8 km × 8 km study area. As our focus was on the spatial variability in LSP, we calculated the mean of SOS and EOS across the six years for each pixel within the study area to obtain pixel-wise mean phenological metrics.

Out of the 26 available foliar functional traits, we selected seven as potential explanatory variables to explain the phenological variability, including LMA, leaf nitrogen content, leaf carbon content, chlorophyll concentration, phenolics concentration, starch concentration and $\delta^{13}C$ (Table 2). These traits are indicative of plant characteristics and their strategies for interacting with the environment. The 1-m trait maps were aggregated to generate trait maps with a 30 m resolution, and the value of the output pixel is the mean of the values of the input 30 × 30 pixels. To obtain trait data with high confidence, we used the maps of trait uncertainties to filter out pixels with uncertainties > 25%, following Wang *et al* (2020).

2.3.2 Generating structural traits from LiDAR data

We derived five structural metrics from the normalized LiDAR point clouds (Table 2). These structural traits include mean canopy height, entropy, height skew, plant area index (PAI), and rugosity. For all tiles of normalized point clouds within the 8 km × 8 km study area, we first

For Peer Review

generated canopy height models (CHM) with a 1 m spatial resolution using the "rasterize_canopy" function from the lidR package (Roussel *et al.*, 2020). Mean canopy height and rugosity were then obtained with the 1-m CHM. Mean canopy height at a 30 m resolution was calculated by averaging canopy height of all pixels within a 30 m × 30 m grid, while rugosity was determined as the standard deviation of all canopy height values within a 30 m × 30 m grid, representing the horizontal spatial heterogeneity within the canopy. Entropy, height skew, and PAI, were directly derived from the point cloud data. Entropy is a normalized Shannon vertical complexity index, quantifying the diversity and evenness of an elevational distribution of points across the 1-m tall slices. Height skew is the skewness of all height values. PAI is the projected area of plant material, including leaves and branches, per unit of ground area. In this study, we computed the total PAI as the sum of the entire plant area density (PAD) vertical profile, estimated using the "lad.voxels" function from the leafR package (de Almeida *et al*., 2021). These three structural traits were computed from regularly segmented LiDAR data at 30 m intervals, resulting in derived structural trait maps having a 30 m spatial resolution, which aligns with the resolution of other datasets.

2.3.3 Data quality control

As the research object of this study is natural vegetation, it is essential to eliminate irrelevant data before conducting further data analysis. To achieve this, we used a land cover map to filter out pixels designated as "Cultivated Cropland", "Barren Land", and "Developed". This step enabled us to exclude non-vegetated areas and vegetation impacted by human activities. However, since misclassified pixels may be present in the land cover map, we also employed PlanetScope-derived NDVI data to further remove non-vegetated areas. We initially derived 3-m NDVI data for each site from PlanetScope images captured during the peak growing season. Then, we generated 30-m NDVI data by aggregating the original NDVI data and using the mean NDVI to align with the resolution of other datasets. Pixels with NDVI value lower than 0.65 were identified and excluded from the subsequent analysis. Since the multi-source data was processed separately to obtain high-quality data, the remaining data pixels vary among different data sources. To ensure the consistency among data from these sources, we identified and selected the common portion of the remaining data pixels across all datasets for further analysis.

2.3.4 Data analysis

For Peer Review

To investigate the differences in phenology among various PFTs at each site, we conducted a one-way analysis of variance (ANOVA) and a least significant difference (LSD) post-hoc test for site-specific data. To ensure that each PFT has enough samples, we only kept PFTs that occupy more than 5% area of the total vegetated area based on the land cover data. We first used the pre-processed phenology dataset in conjunction with land cover maps to calculate the mean SOS and EOS for each PFT by averaging the phenological metrics of all pixels within the same PFT. We then compared the PFT-specific mean phenological metrics using the one-way ANOVA and LSD post-hoc test, allowing us to assess the significance of the differences in phenology among these PFTs.

To further quantify the contribution of PFTs in explaining site-level phenological variability, we employed an ANOVA-based general linear model (Guillén-Escribà *et al.*, 2021; Liu *et al.*, 2023). This approach enabled us to decompose the site-level phenological variability into inter-PFT and intra-PFT components. We first fitted a general linear model with the PFT term and then partitioned the total variance of site-level phenology into inter-PFT (PFT term) and intra-PFT (residual) components by calculating the percentage of sum of squares explained by the PFT term. The inter-PFT component indicates the variance of phenology that could be explained by PFTs alone.

Boosted regression trees (BRTs; Elith, Leathwick, & Hastie, 2008) were employed to explore whether plant functional traits could enhance our understanding of intra-site phenological variability. BRTs are an effective tool for analysing datasets with numerous predictors, as they combine the decision tree algorithm with the boosting method. This approach can model non-linear relationships and interactions among various continuous and categorical predictors and is relatively insensitive to collinearity among predictors. Additionally, BRTs can automatically handle the missing values in datasets, making them suitable for analysing large quantities of data. In this study, we built site-specific BRT models for SOS and EOS, respectively, as our study sites are located in different latitudinal regions with varying climatic conditions, leading to significant inter-site phenological variation. For each BRT model, the pixel-level SOS/EOS served as the response variable, while the plant functional traits were the explanatory variables. We fitted all BRT models using the R package “dismo” (Hijmans *et al.*, 2023) with the same parameter settings and procedure. These specific parameter settings include a Gaussian error distribution, a fraction of training data (bag fraction) of 0.5, a tree complexity of 5, and a learning rate of 0.05. We also employed a 10-fold cross-validation procedure to minimize overfitting and obtain the optimized number of trees. The cross-validation correlation (cv) was

For Peer Review

used as an indicator to evaluate model performance. Moreover, BRTs provide the relative importance of each predictor on the dependent variable, which is helpful in assessing which plant functional traits are important in regulating the intra-site phenological variability.

To obtain a general relationship between multivariate functional traits and phenology across different study sites, we conducted a principal component analysis (PCA) using seven leaf functional traits and five structural traits from all study sites. We employed the R package "FactoMineR" (Husson *et al*., 2023) for the PCA analysis, and all trait data were standardized using the "scale" function in R prior to the analysis. The top three derived principal components (PCs) explained 62.8% of the total variance in the data, capturing the major coordination among different traits and indicating trade-offs among various plant adaptive strategies. We performed a correlation analysis between dominant PCs and phenological metrics for data from each site separately. This analysis sought to improve our understanding of whether there are any adaptive strategies that regulate the intra-site phenological variability across the study sites. All the data analysis were conducted in R 4.2.0 (R Core Team, 2023).

3. Results

3.1. Variation in phenology across and within PFTs at the intra-site level

Our analysis of phenological variation within each study site revealed considerable variation at both inter- and intra-PFT levels (Figs. 2-3). Distinct phenological patterns were evident when visually comparing the PFT maps with the maps of mean SOS and EOS from 2016 to 2021 (Fig. 2), and the quantitative analysis of phenological metrics across PFTs also demonstrated significant differences in these metrics among PFTs at each site (Fig. 3, Table S1). For instance, at the SERC site, hay/pasture displayed earlier SOS (mean DOY = 109) and EOS (mean DOY = 285) than deciduous forest (SOS: mean DOY = 113; EOS: mean DOY = 293). At the TREE and UNDE sites, wetlands exhibited later SOS and earlier EOS compared to deciduous and mixed forests (Table S1). We also observed substantial intra-PFT phenological variation at the DELA site, with both hay/pasture and woody wetlands displaying considerable variation (Table S1). Despite the observed inter-PFT variation, the ranges of SOS and EOS across PFTs at each site exhibited considerable overlaps, with minor intra-site phenological variation (0.8% to 23.4%) attributable to PFTs (Figs. 3-4). Specifically, PFTs accounted for 3.2% and 0.8% of the variation in SOS and EOS, respectively, at the DELA site, whereas at the SERC site, PFTs accounted for 7.7% of the SOS variation and 3.8% of the EOS variation. In contrast, over 13%

For Peer Review

of the variation in phenological metrics at the TREE and UNDE sites was explained by PFTs. Overall, these results demonstrate that inter-PFT variation accounted for a relatively small fraction of the total variation in SOS and EOS, with the majority of the variability (76.6% to 99.2%) arising from intra-PFT variation.

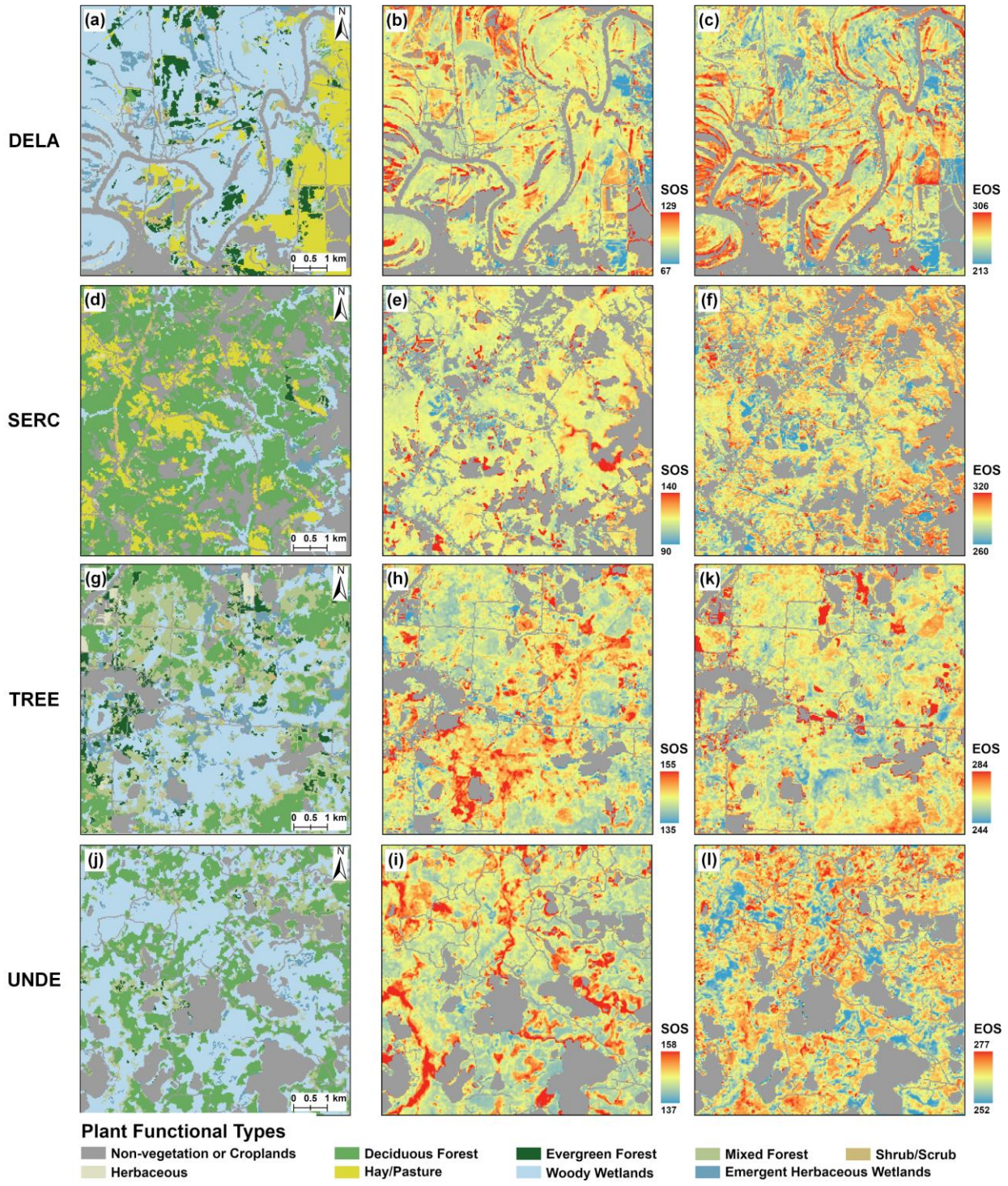

Fig. 2. Maps of plant functional types and mean phenological metrics from 2016 to 2021 for four study sites. (a, d, g, j) Maps of plant functional types at the DELA, SERC, TREE, and

UNDE sites, respectively; (b, e, h, i) Maps of mean SOS from 2016 to 2021 of the DELA, SERC, TREE, and UNDE sites, respectively; (c, f, k, l) Maps of mean EOS from 2016 to 2021 of the DELA, SERC, TREE, and UNDE sites, respectively.

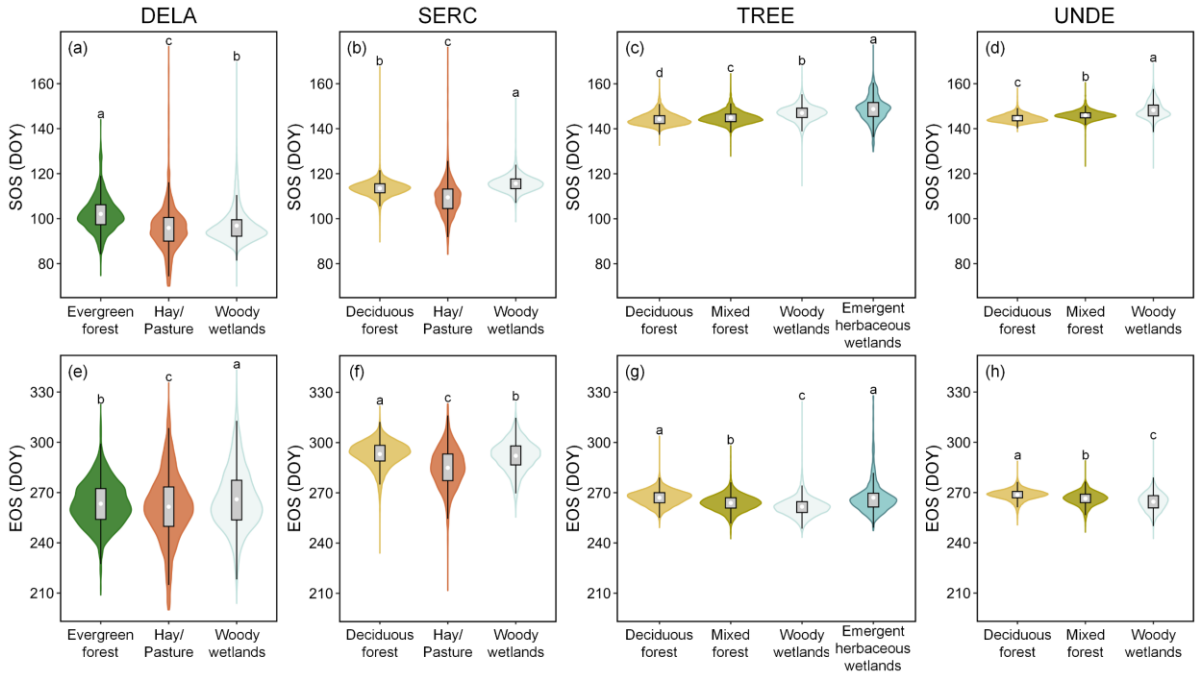

Fig. 3. Comparisons of SOS and EOS across plant functional types (PFTs) at each study site. The white circles and the boxes within each violin plot represent the mean values and the 95% confidence intervals, and the whiskers in each violin plot indicate the range. Different lower-case letters adjoining the violin plots indicate significant differences (p<0.05) among PFTs for the phenological metrics, based on one-way ANOVA with the least significant difference post-hoc test. Panels (a) and (e) show the SOS and EOS of the dominant PFTs at the DELA site. Panels (b) and (f) show the SOS and EOS of the dominant PFTs at the SERC site. Panels (c) and (g) show the SOS and EOS of dominant PFTs at the TREE site. Panels (d) and (h) show the SOS and EOS of dominant PFTs at the UNDE site.

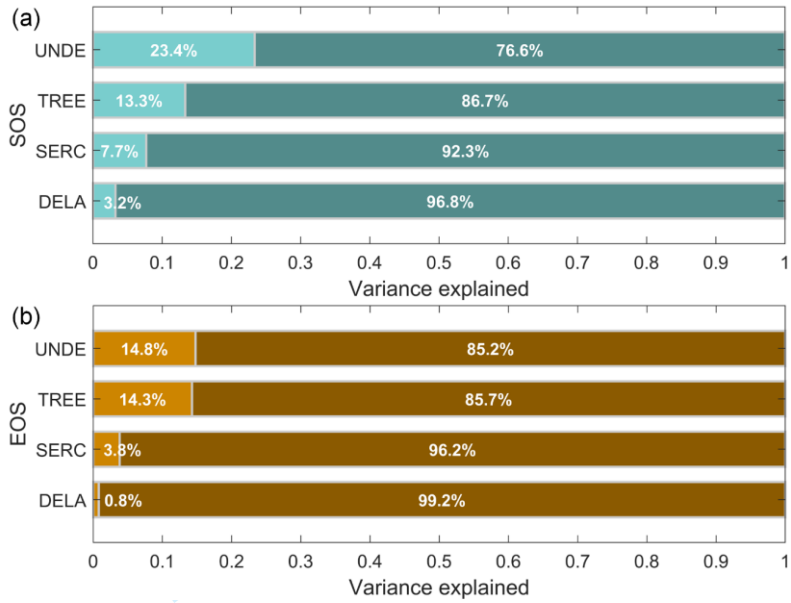

Fig. 4. Variance partitioning of (a) SOS and (b) EOS at each study site. The total variability of SOS and EOS was partitioned into the inter-PFT and intra-PFT components. The light cyan and brown bars indicate the inter-PFT component of the variances of SOS and EOS respectively, while dark cyan and brown bars indicate the intra-PFT component of the variances of SOS and EOS respectively.

3.2. The influence of plant functional traits on phenological variation at the intra-site level

Our results from BRT models demonstrated that the involved functional traits provided enhanced explanatory power for intra-site phenological variation consistently across all sites, with the cross-validation correlation ranging from 0.50 to 0.85 for SOS and from 0.58 to 0.77 for EOS (Fig. 5; Figs. S2-S9). The BRT models also revealed variability in the role of different functional traits in regulating intra-site SOS *vs.* EOS variation within the same site, as well as considerable differences in the contribution of functional traits to intra-site variation of the same phenological metric across the four sites. Despite these differences, we observed some similarities in the contribution of functional traits to phenological variation across all the sites. Specifically, we found that LMA, canopy height and PAI were strongly associated with SOS, with LMA accounting for 7.47% to 13.15%, canopy height accounting for 9.83% to 28.46%, and PAI accounting for 4.87% to 11.64% of the total contribution. Similarly, carbon content, canopy height, and $\delta^{13}C$ were important for explaining EOS variation, with carbon content accounting for 5.35% to 20.60%, $\delta^{13}C$ accounting for 5.86% to 15.90%, and canopy height accounting for 6.34 % to 45.70% of the total contribution. In contrast, entropy and rugosity had a less impact on variation in both SOS and EOS. The importance of phenolics concentration differed across sites, being significant for the DELA (11.29% for SOS, 11.03% for EOS),

401 TREE (10.31% for SOS, 10.38% for EOS), and UNDE (9.84% for SOS, 8.06% for EOS) sites,
402 but not for the SERC site (5.19% for SOS, 3.33% for EOS). Other functional traits, including
403 height skew, chlorophyll concentration, nitrogen content, and starch concentration exhibited
404 varying explanatory importance for the variation in SOS and EOS across the four sites.

405 We further grouped the functional traits into four groups based on their ecological meaning
406 and calculated the relative contributions of each group to the explained phenological variation
407 (Fig.5). Group 1, comprised of canopy height, height skew, and PAI, relates to the amount and
408 distribution of vegetation biomass. Group 2, consisting of entropy and rugosity, is associated
409 with the spatial heterogeneity of vegetation. Group 3 includes carbon, chlorophyll, LMA,
410 nitrogen, and $\delta^{13}C$, which are connected to the metabolic strategies of vegetation. Group 4
411 contains phenolics and starch, which are linked to plant strategies in response to environmental
412 stress and disturbances. We found that Group 1 and Group 3 were crucial in explaining
413 variation in both SOS and EOS, with Group 1 accounting for between 17.83% to 55.91% and
414 Group 3 accounting for between 28.28% to 55.58% of the overall contribution, whereas Group
415 2 and Group 4 played a less significant role, with Group 2 responsible for approximately 10%
416 and Group 4 accounting for about 15% of the overall contribution.

For Peer Review

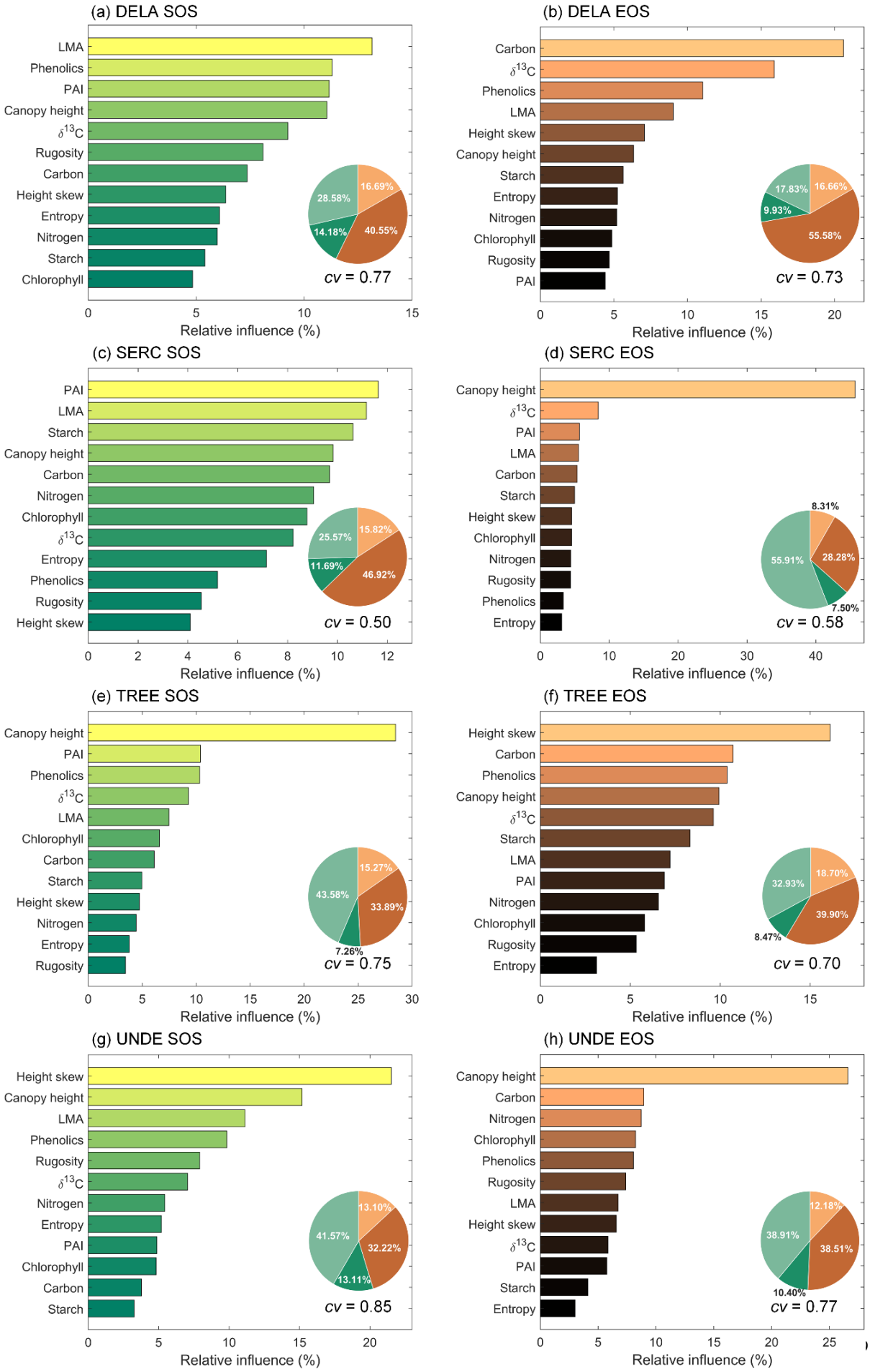
(a) DELA SOS
LMA
Phenolics
PAI
Canopy height
δ13C
Rugosity
Carbon
Height skew
Entropy
Nitrogen
Starch
Chlorophyll
16.69%
28.58%
14.18%
40.55%
cv = 0.77
Relative influence (%)
(b) DELA EOS
Carbon
δ13C
Phenolics
LMA
Height skew
Canopy height
Starch
Entropy
Nitrogen
Chlorophyll
Rugosity
PAI
17.83%
16.66%
9.93%
55.58%
cv = 0.73
Relative influence (%)
(c) SERC SOS
PAI
LMA
Starch
Canopy height
Carbon
Nitrogen
Chlorophyll
δ13C
Entropy
Phenolics
Rugosity
Height skew
25.57%
15.82%
11.69%
46.92%
cv = 0.50
Relative influence (%)
(d) SERC EOS
Canopy height
δ13C
PAI
LMA
Carbon
Starch
Height skew
Chlorophyll
Nitrogen
Rugosity
Phenolics
Entropy
8.31%
55.91%
28.28%
7.50%
cv = 0.58
Relative influence (%)
(e) TREE SOS
Canopy height
PAI
Phenolics
δ13C
LMA
Chlorophyll
Carbon
Starch
Height skew
Nitrogen
Entropy
Rugosity
15.27%
43.58%
33.89%
7.26%
cv = 0.75
Relative influence (%)
(f) TREE EOS
Height skew
Carbon
Phenolics
Canopy height
δ13C
Starch
LMA
PAI
Nitrogen
Chlorophyll
Rugosity
Entropy
18.70%
32.93%
39.90%
8.47%
cv = 0.70
Relative influence (%)
(g) UNDE SOS
Height skew
Canopy height
LMA
Phenolics
Rugosity
δ13C
Nitrogen
Entropy
PAI
Chlorophyll
Carbon
Starch
13.10%
41.57%
32.22%
13.11%
cv = 0.85
Relative influence (%)
(h) UNDE EOS
Canopy height
Carbon
Nitrogen
Chlorophyll
Phenolics
Rugosity
LMA
Height skew
δ13C
PAI
Starch
Entropy
12.18%
38.91%
38.51%
10.40%
cv = 0.77
Relative influence (%)

Fig. 5. Relative importance (%) of plant functional traits on SOS (a, c, e, g) and EOS (b, d, f, h) of each study site, deduced from boosted regression trees (BRTs). BRT models were fitted for (a) SOS at DELA (cross-validation correlation (cv) = 0.77), (b) EOS at DELA (cv = 0.73), (c) SOS at SERC (cv = 0.50), (d) EOS at SERC (cv = 0.58), (e) SOS at TREE (cv = 0.75), (f) EOS at TREE (cv = 0.70), (g) SOS at UNDE (cv = 0.85), (h) EOS at UNDE (cv = 0.77). LMA, leaf mass per area; PAI, plant area index. Pie charts represent the overall contributions of functional traits, grouped by their ecological meaning, deduced from the BRT models. Light green represents the contribution of Group 1 (canopy height, height skew, and PAI). Dark green represents the contribution of Group 2 (entropy and rugosity). Dark orange represents the contribution of Group 3 (carbon, chlorophyll, LMA, nitrogen, and $\delta^{13}C$). Light orange represents the contribution of Group 4 (phenolics and starch).

3.3. The relationship between multivariate functional traits and phenological metrics

The results from PCA analysis showed that the first three principal components (PCs) accounted for 26.6% (PC1), 21.3% (PC2), and 14.9% (PC3) of the total trait variation, respectively (Fig. 6). Among these PCs, PC1 was predominantly associated with structural traits related to the amount and distribution of vegetation biomass. Vegetation with large canopy height, PAI, and top-skewed canopies exhibited positive values on PC1. PC2 was primarily linked to LMA, nitrogen content, carbon content, and $\delta^{13}C$. Vegetation with high LMA and carbon content, low nitrogen content and $\delta^{13}C$, had positive value on this axis. PC3 was mainly related to functional traits associated with plant defense and response to environmental stress and disturbances, including phenolics and starch concentration.

We further investigated the relationship between phenological metrics and the PCs by conducting the Pearson correlation analysis at the intra-site level. This analysis revealed that PC1 was negatively correlated with SOS at DELA, TREE, and UNDE sites, with r ranging from -0.52 to -0.38 (Table 3). Similarly, SOS for different PFTs at these three sites also exhibited negative associations with PC1 (Table S2). This suggests that most vegetation with large canopy height, PAI, and top-skewed canopies at these sites tend to have earlier SOS. In contrast, PC1 showed a positive correlation with EOS for most sites and PFTs (Tables 3 and S2). PC2 was positively associated with SOS at all sites, but to varying degrees (r = 0.02-0.38). This axis displayed negative correlations with EOS at DELA (r = -0.30), TREE (r = -0.34), and UNDE (r = -0.41) sites, and a weak positive correlation with EOS at the SERC site (r = 0.05). These results suggest that vegetation with high LMA and carbon content, low nitrogen content and $\delta^{13}C$ at these sites generally have later SOS and earlier EOS. PC3 was positively

For Peer Review

related to SOS at the DELA (r = 0.11) and SERC (r = 0.23) sites while negatively associated with SOS at the TREE (r = -0.17) and UNDE (r = -0.26) sites. This axis exhibited positive relationships with EOS, except for the SERC site (r = -0.03). Across PFTs from different sites, PC3 showed more varied relationships with phenological metrics compared to PC1 and PC2 (Table S2).

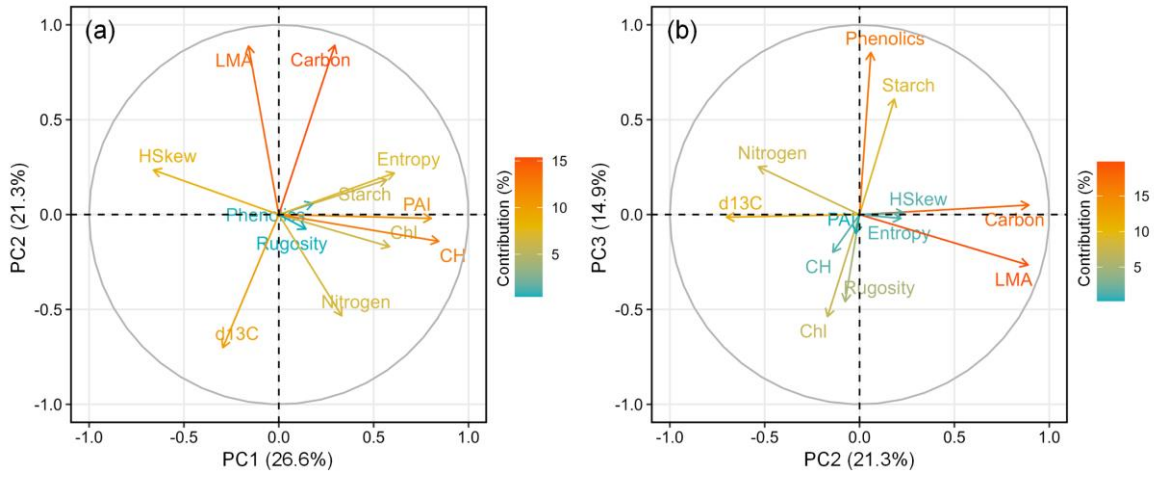

Fig. 6. Principal component analysis (PCA) for 12 plant functional traits across all study sites. (a) Trait loadings along the first (PC1) and second (PC2) principal components. (b) Trait loadings along the PC2 and the third (PC3) principal component. Arrows are colored according to the contribution of traits to the principal components. PC1, PC2, and PC3 explained 26.6%, 21.3%, and 14.9% of the total variation in 12 plant functional traits, respectively. CH, canopy height; Chl, chlorophyll concentration; d13C, $\delta^{13}C$; HSkew, height skew; LMA, leaf mass per area; PAI, plant area index.

Table 3. Correlation coefficients between main principal components and phenological metrics of each study site.

Site	Phenological metrics	PC1	PC2	PC3
DELA	SOS	-0.38	0.12	0.11
	EOS	-0.29	-0.30	0.15
SERC	SOS	0.13	0.26	0.23
	EOS	0.40	0.05	-0.03
TREE	SOS	-0.52	0.02	-0.17
	EOS	0.20	-0.34	0.18
UNDE	SOS	-0.52	0.38	-0.26
	EOS	0.30	-0.41	0.11

Note: All the correlations are statistically significant with p<0.001.

4. Discussion

Understanding the role of biotic factors in regulating phenological variation is important for comprehending the underlying mechanisms and drivers of this variation. In this study, we evaluated the influence of PFTs and plant functional traits on explaining LSP variation across four landscapes with minor topographic relief. Our results show considerable intra-site phenological variability across all four study sites, with biotic factors significantly contributing to this variability. PFTs alone have limited explanatory power for phenological variability, while plant functional traits contribute more significantly. Among various traits examined in this study, those related to competitive ability and productivity are particularly important for explaining intra-site phenological variability, although their relative contributions vary across sites. Moreover, the relationships between major principal components derived from multiple functional traits suggest potential plant strategies for regulating such phenological variation. Collectively, these results demonstrate that biotic factors play an important role in regulating phenological variability in addition to climatic factors.

4.1. Considerable intra-site phenological variability and the limited explanatory power of PFTs alone

Climatic factors are well-established as dominant drivers of phenological variability across vegetated landscapes spanning large environmental gradients. To minimize the influence of intra-site climatic variation, we selected sites with minor topographic relief. However, significant phenological variation still persists within each site (Figs. 2-3; Table S1), with intra-site variation of more than 20 days in SOS and more than 25 days in EOS across all four sites. Within each site, three to four dominant PFTs were observed, and the contribution of PFTs to explain intra-site phenological variability was confirmed (Fig. 4). However, since PFTs are broadly categorized based on plant functional characteristics, it is not surprising that PFTs alone play a limited role in explaining intra-site phenological variability. The contribution of PFTs in explaining phenological variability has also been demonstrated in recent studies (Misra *et al.*, 2018; Wang *et al.*, 2021). In addition, the explanatory contribution of PFTs across different sites can be influenced by the variation in PFT's relative abundance at each site. For example, the TREE and UNDE sites with higher PFT contributions exhibit a more even distribution of different PFTs compared to the DELA and SERC sites, which are dominated by only one dominant PFT (Table S3). Regardless, the large intra-PFT phenological variability observed in Fig. 4 indicates that PFTs alone are insufficient to describe the intra-site LSP variability, suggesting that other biotic factors or processes play a more significant role.

For Peer Review

4.2. Plant functional traits importantly regulate intra-site phenological variability

Our results show that incorporating key traits significantly improves the explanatory power (Fig. 5) across all four sites compared to using only PFTs (Fig. 4). This improvement can be attributed to functional traits providing a more detailed characterization of plant biochemical and biophysical attributes than PFTs, which allows for better differentiation of growth forms, species, and individuals that ultimately contribute to intra-site phonological variation. For example, LMA values differ significantly between tree and herbaceous species, as well as evergreen and deciduous species (Poorter *et al.*, 2009). Moreover, plant phenolics concentration, PAI, and canopy height have been shown to be important for distinguishing co-existing species (Asner *et al.*, 2012), representing forest composition (Hwang *et al.*, 2011), and reflecting the variation between age classes within a forest community (de Souza & da Costa, 2020), respectively. By considering these multiple functional traits, we were able to achieve a more comprehensive representation of plant features, which better characterize different species and individuals, and ultimately lead to an improved interpretation of intra-site phenological variability.

The BRT models identified that LMA, canopy height, and PAI emerged as dominant traits for explaining SOS variation, while carbon content, canopy height, and $\delta^{13}C$ were important for explaining EOS variation (Fig. 5). Both canopy height and LMA are associated with plant productivity and competitive ability, and their variations may reflect inter- and intra-specific responses to environmental conditions (Poorter *et al.*, 2009; Huang *et al.*, 2018). Previous studies have also suggested significant impacts of these two traits on plant phenology within a few field sites (Osada, 2017; Adams *et al.*, 2021; Liu *et al.*, 2021; Sporbert *et al.*, 2022). Furthermore, canopy height and PAI can influence microclimatic conditions, such as temperature and light availability (Jucker *et al.*, 2018; De Frenne *et al.*, 2021), which can affect the occurrence of phenological events (Fisher *et al.*, 2006; Klosterman & Richardson, 2017). $\delta^{13}C$ serves as a useful proxy for plant water use efficiency, while leaf senescence timing has often been viewed as a drought and water stress coping strategy (Blumenthal *et al.*, 2020; Brum *et al.*, 2023), making $\delta^{13}C$ an effective indicator of plant responses to water stress and EOS timing regulation (Bucher & Römermann, 2021). These findings collectively suggest that plant functional traits, particularly those related to productivity, competitive ability, and metabolic strategies, play a critical role in regulating intra-site phenological variability. Besides the common traits identified across all four sites for explaining intra-site phenological variability, we also observed considerable variation in the relative importance of these traits (Fig. 5). This

For Peer Review

variation likely arises from the site-specific environmental factors and differences in species composition (McGill *et al.*, 2006; Messier *et al.*, 2017), however, further research is needed to better understand the complex relationships between plant functional traits and phenological patterns in different forest ecosystems.

4.3. Potential strategies underlying plant phenological variability

The significant impact of functional traits on intra-site phenological variability suggests the potential ecological strategies underlying plant phenology regulation. To explore these strategies, we conducted a PCA analysis to reduce collinearity among functional traits (Fig. S1) and analyzed the relationships between the first three PCs (Fig. 6) and phenological metrics.

PC1, related to canopy height, height skew, and PAI, may indicate a carbon balance strategy. It correlates negatively with SOS but positively with EOS for most sites and PFTs (Tables 3 and S2). These relationships imply that taller, denser plant canopies have earlier SOS and delayed EOS. This finding contradicts previous observations that suggest shorter understory vegetation displays earlier leaf emergence and later senescence to avoid light competition with canopy trees (Seiwa, 1999; Osada & Hiura, 2019), but it aligns with studies that focus on upper canopy trees (Ding *et al.*, 2020; Adams *et al.*, 2021), which is our primary focus. The rationale could be that larger trees incur a higher carbon cost and necessitate a longer growth period to maintain carbon balance (Blonder *et al.*, 2023). However, a recent study with field observations revealed that the relationship between vegetation height and phenology could vary across species (Marchand et al., 2020). Our results, combined with previous studies, suggest that a strategy involving canopy structure drives plant phenological variability, and this relationship may vary across species, and further research is needed to improve our understanding.

PC2, mainly associated with LMA, carbon, nitrogen, and $\delta^{13}C$, indicates an integrated resource use strategy and correlates positively with SOS and negatively with EOS. This finding suggests that plant canopies with higher photosynthetic capacity (lower LMA, higher nitrogen content) and higher water use efficiency (higher $\delta^{13}C$; Condon *et al.*, 2002) tend to have earlier SOS and delayed EOS. This is inconsistent with the leaf economic spectrum theory (LES; Reich *et al.*, 1997; Wright *et al.*, 2004), which is supported by several leaf-level studies (Liu *et al.*, 2011; Sun *et al.*, 2006), stating that vegetation with higher leaf construction cost and/or lower photosynthetic capacity (larger LMA and lower nitrogen content) would have earlier SOS and later EOS to extend the photosynthetic period. This inconsistency could be due to the scale mismatch between our canopy-scale observations and the leaf-scale LES theory, and the

For Peer Review

longevity of a single leaf may differ from the full growing season length derived from satellite data. Similarly, some studies also found that plants with smaller LMA are associated with earlier SOS and delayed EOS (Osada, 2017; Liu *et al.*, 2021). This could also be because LES trait correlations are not always consistent with the theory at local scales or within plant canopies, indicating that plants adopt context-dependent resource use strategy to maximize the whole plant photosynthesis (Baldocchi *et al.*, 2002; Niinemets & Valladares, 2004; Anderegg *et al.*, 2018).

PC3, mainly associated with phenolics and starch, indicates a defensive strategy (Kokaly & Skidmore, 2015; Wang *et al.*, 2022). This PC displays complex and varied relationships with phenological metrics across sites. For example, at the two northern sites (TREE and UNDE), PC3 tends to negatively correlate with SOS and positively with EOS, whereas the relationships are somewhat opposite and more intricate at the two southern sites (DELA and SERC). This pattern may arise because the defensive strategy is more effective in cold regions, allowing vegetation with stronger defensive ability (larger PC3) to better cope with environmental stress (Stark *et al.*, 2015; Naikoo *et al.*, 2019; Ribeiro *et al.*, 2022). However, the mechanism underlying this strategy's role in regulating plant phenology remains unclear, and further in-depth analysis is needed in future research.

4.4. Uncertainties and future directions

We identify several uncertainties that may impact our interpretation of results. First, the accuracy of phenology and functional trait data used in this study could be affected by various factors. Although we used multi-year averaged phenology data from HLS, which has shown high accuracy in previous studies (Bolton *et al.*, 2020; Moon *et al.*, 2021a), uncertainties may exist in the phenology data due to potential limitations in data quality. For plant functional traits, despite the high accuracy of airborne imagine spectroscopy for trait mapping, our remotely derived trait data could have uncertainties, especially in regions with insufficient sampling (Wang *et al.*, 2020). Moreover, airborne LiDAR systems produce uneven data distribution along the vertical profile (LaRue *et al.*, 2020), potentially introducing uncertainties in derived structural traits. These uncertainties may lead to the underestimation of the role of foliar and structural traits in explaining intra-site phenological variability. Second, while we minimized the effect of intra-site climate variation on phenological variability by selecting sites with minor topographic relief, other variables related to microclimate, soil moisture, and nutrient availability may still cause intra-site phenological variability (Hwang *et al.*, 2011; Elmore *et al.*, 2012; Wang *et al.*, 2023) and warrant further investigation. Third, due to the lack

For Peer Review

of certain trait data, such as wood density and xylem traits, which have been previously suggested as important traits for phenology (Yin *et al.*, 2016; Adams *et al.*, 2021), our analysis may overlook certain biotic mechanisms regulating intra-site phenological variability.

Our study also identifies at least two steps for future advances. First, incorporating species and phylogeny data into the analysis could help elucidate the mechanisms behind intra-site phenological variation. Since functional traits differ among species and phylogenetically distant clades (Messier *et al.*, 2010; Furey & Tilman, 2023; Yan *et al.*, 2023), combining species and phylogeny data with functional traits could better explain phenological variation from both intraspecific and interspecific components (Klosterman & Richardson, 2017; Klosterman *et al.*, 2018). The recent availability of remote sensing data for species identification and mapping (Xu *et al.*, 2020; Mäyrä *et al.*, 2021; Marconi *et al.*, 2022) could facilitate this exploration. Moreover, ecosystem-scale phenology models currently have considerable uncertainties due to inadequate observations and limited knowledge regarding the mechanisms of individual- and species-scale phenology (Tang et al., 2016). With the combination of species and functional trait data, we can improve our understanding of the phenological responses of individual plants and species within a community to environmental conditions, which may advance the development of ecosystem-scale phenology models. Second, considering other environmental factors, such as microclimate and soil properties, could help explain intra-site phenological variation (Klosterman & Richardson, 2017; Yang *et al.*, 2023). Although accurate large-scale data for these factors are currently lacking, remote sensing techniques and field measurements could be combined to obtain high accuracy data at large spatial extents (Davis *et al.*, 2019; Peng *et al.*, 2021). In addition to the above investigations, studying the interactions among environmental factors, vegetation, and phenology could lead to a more comprehensive understanding of the mechanisms underlying intra-site phenological variation.

For Peer Review

Acknowledgements

This work was supported by National Natural Science Foundation of China (#31922090) and Hong Kong Research Grant Council General Research Fund (#17305321). J. Wu was also supported by the HKU Seed Funding for Strategic Interdisciplinary Research Scheme, Hong Kong Research Grant Council Collaborative Research Fund (#C5062-21GF), and the Innovation and Technology Fund (funding support to State Key Laboratories in Hong Kong of

Agrobiotechnology) of the HKSAR, China. Z.W. was funded by GDAS' Special Project of Science and Technology Development (2020GDASYL-20200102001). M.M was supported by NASA grants #80NSSC21K1974. D.Y. was supported by the United States Department of Energy contract No. DE-SC0012704 to Brookhaven National Laboratory. J. Wang was supported by Shenzhen Science and Technology Program (Grant No. 20220816162849005). The National Ecological Observatory Network (NEON) is a program sponsored by the National Science Foundation and operated under cooperative agreement by Battelle. This material is based in part upon work supported by the National Science Foundation through the NEON Program.

Competing interests

None.

Author contributions

YZ and J Wu conceived the study. YZ designed the analyses with inputs from J Wu, ZW and ZY. YZ performed the analyses. MM provided the land surface phenology data from 2020 to 2021. All authors contributed to interpreting the results. YZ drafted the manuscript with constructive input from J Wu, and all authors contributed to the manuscript editing.

Data availability

Multi-Source Land Surface Phenology (MSLSP) product is available at https://lpdaac.usgs.gov/products/mslsp30nav011/, foliar functional trait data are available at https://tinyurl.com/neontraits1, LiDAR point cloud data are available at https://doi.org/10.48443/xxby-5a18, the land cover map from United States Geological Survey's (USGS) National Land Cover Database (NLCD) for the year 2019 is available at https://doi.org/10.5066/P9KZCM54.

References

Adams BT, Matthews SN, Iverson LR, Prasad AM, Peters MP, Zhao K. 2021. Spring phenological variability promoted by topography and vegetation assembly processes in a

For Peer Review

temperate forest landscape. *Agricultural and Forest Meteorology* **308–309**: 108578.

de Almeida D, Stark S, Silva C, Hamamura C, Valbuena R. 2021. leafR: Calculates the Leaf Area Index (LAD) and Other Related Functions. [WWW document] URL https://github.com/DRAAlmeida/leafR [accessed 24 August 2023].

Anderegg LDL, Berner LT, Badgley G, Sethi ML, Law BE, HilleRisLambers J. **2018**. Within-species patterns challenge our understanding of the leaf economics spectrum. *Ecology Letters* **21**: 734–744.

Asner GP, Martin RE, Anderson CB, Knapp DE. **2015**. Quantifying forest canopy traits: Imaging spectroscopy versus field survey. *Remote Sensing of Environment* **158**: 15–27.

Asner GP, Martin RE, Suhaili A Bin. **2012**. Sources of Canopy Chemical and Spectral Diversity in Lowland Bornean Forest. *Ecosystems* **15**: 504–517.

Baldocchi DD, Wilson KB, Gu L. **2002**. How the environment, canopy structure and canopy physiological functioning influence carbon, water and energy fluxes of a temperate broad-leaved deciduous forest - An assessment with the biophysical model CANOAK. *Tree Physiology* **22**: 1065–1077.

Blonder BW, Brodrick PG, Chadwick KD, Carroll E, Cruz-de Hoyos RM, Expósito-Alonso M, Hateley S, Moon M, Ray CA, Tran H, *et al.* 2023. Climate lags and genetics determine phenology in quaking aspen (Populus tremuloides). *New Phytologist* **238**: 2313–2328.

Blumenthal DM, Mueller KE, Kray JA, Ocheltree TW, Augustine DJ, Wilcox KR. **2020**. Traits link drought resistance with herbivore defence and plant economics in semi-arid grasslands: The central roles of phenology and leaf dry matter content. *Journal of Ecology* **108**: 2336–2351.

Bolton DK, Gray JM, Melaas EK, Moon M, Eklundh L, Friedl MA. **2020**. Continental-scale land surface phenology from harmonized Landsat 8 and Sentinel-2 imagery. *Remote Sensing of Environment* **240**: 111685.

Brum M, Vadeboncoeur M, Asbjornsen H, Vilca BLP, Galiano D, Horwath AB, Metcalfe DB. **2023**. Ecophysiological controls on water use of tropical cloud forest trees in response to experimental drought. *Tree Physiology* **tpad070**.

Bucher SF, Feiler R, Buchner O, Neuner G, Rosbakh S, Leiterer M, Römermann C.

For Peer Review

2019. Temporal and spatial trade-offs between resistance and performance traits in herbaceous plant species. *Environmental and Experimental Botany* **157**: 187–196.

Bucher SF, König P, Menzel A, Migliavacca M, Ewald J, Römermann C. **2018**. Traits and climate are associated with first flowering day in herbaceous species along elevational gradients. *Ecology and Evolution* **8**: 1147–1158.

Bucher SF, Römermann C. **2021**. The timing of leaf senescence relates to flowering phenology and functional traits in 17 herbaceous species along elevational gradients. *Journal of Ecology* **109**: 1537–1548.

Charrier G, Ngao J, Saudreau M, Améglio T. **2015**. Effects of environmental factors and management practices on microclimate, winter physiology, and frost resistance in trees. *Frontiers in Plant Science* **6**: 259.

Cleland EE, Chuine I, Menzel A, Mooney HA, Schwartz MD. **2007**. Shifting plant phenology in response to global change. *Trends in Ecology and Evolution* **22**: 357–365.

Cole EF, Sheldon BC. **2017**. The shifting phenological landscape: Within- and between-species variation in leaf emergence in a mixed-deciduous woodland. *Ecology and Evolution* **7**: 1135–1147.

Condon AG, Richards RA, Rebetzke GJ, Farquhar GD. **2002**. Improving intrinsic water-use efficiency and crop yield. *Crop Science* **42**: 122–131.

Croft H, Chen JM, Froelich NJ, Chen B, Staebler RM. **2015**. Seasonal controls of canopy chlorophyll content on forest carbon uptake: Implications for GPP modeling. *Journal of Geophysical Research G: Biogeosciences* **120**: 1576–1586.

Dahlin KM, Asner GP, Field CB. **2013**. Environmental and community controls on plant canopy chemistry in a Mediterranean-type ecosystem. *Proceedings of the National Academy of Sciences of the United States of America* **110**: 6895–6900.

Davis FW, Synes NW, Fricker GA, McCullough IM, Serra-Diaz JM, Franklin J, Flint AL. **2019**. LiDAR-derived topography and forest structure predict fine-scale variation in daily surface temperatures in oak savanna and conifer forest landscapes. *Agricultural and Forest Meteorology* **269–270**: 192–202.

Dawson TE, Mambelli S, Plamboeck AH, Templer PH, Tu KP. **2002**. Stable Isotopes in Plant Eecology. *Annual Review of Ecology and Systematics* **33**: 507–559.

For Peer Review

Delpierre N, Soudani K, Berveiller D, Dufrêne E, Hmimina G, Vincent G. **2020**. "Green pointillism": detecting the within-population variability of budburst in temperate deciduous trees with phenological cameras. *International Journal of Biometeorology* **64**: 663–670.

Dewitz J, USGS, 2021. National Land Cover Database (NLCD) 2019 Products (ver. 2.0, June 2021). https://doi.org/10.5066/P9KZCM54 [accessed 24 August 2023].

Ding C, Hamann A, Yang RC, Brouard JS. **2020**. Genetic parameters of growth and adaptive traits in aspen (Populus tremuloides): Implications for tree breeding in a warming world. *PLoS ONE* **15**: e0229225.

Dragoni D, Rahman AF. **2012**. Trends in fall phenology across the deciduous forests of the Eastern USA. *Agricultural and Forest Meteorology* **157**: 96–105.

Elith J, Leathwick JR, Hastie T. **2008**. A working guide to boosted regression trees. *Journal of Animal Ecology* **77**: 802–813.

Elmore AJ, Guinn SM, Minsley BJ, Richardson AD. **2012**. Landscape controls on the timing of spring, autumn, and growing season length in mid-Atlantic forests. *Global Change Biology* **18**: 656–674.

Van Ewijk KY, Randin CF, Treitz PM, Scott NA. **2014**. Predicting fine-scale tree species abundance patterns using biotic variables derived from LiDAR and high spatial resolution imagery. *Remote Sensing of Environment* **150**: 120–131.

Fisher JI, Mustard JF, Vadeboncoeur MA. **2006**. Green leaf phenology at Landsat resolution: Scaling from the field to the satellite. *Remote Sensing of Environment* **100**: 265–279.

Forrest J, Miller-Rushing AJ. **2010**. Toward a synthetic understanding of the role of phenology in ecology and evolution. *Philosophical Transactions of the Royal Society B: Biological Sciences* **365**: 3101–3112.

De Frenne P, Lenoir J, Luoto M, Scheffers BR, Zellweger F, Aalto J, Ashcroft MB, Christiansen DM, Decocq G, De Pauw K, *et al.* 2021. Forest microclimates and climate change: Importance, drivers and future research agenda. *Global Change Biology* **27**: 2279–2297.

Furey GN, Tilman D. **2023**. Plant chemical traits define functional and phylogenetic axes of plant biodiversity. *Ecology Letters* **26**: 1394–1406.

For Peer Review

Garonna I, de Jong R, de Wit AJW, Mücher CA, Schmid B, Schaepman ME. **2014**. Strong contribution of autumn phenology to changes in satellite-derived growing season length estimates across Europe (1982-2011). *Global Change Biology* **20**: 3457–3470.

Guillén-Escribà C, Schneider FD, Schmid B, Tedder A, Morsdorf F, Furrer R, Hueni A, Niklaus PA, Schaepman ME. **2021**. Remotely sensed between-individual functional trait variation in a temperate forest. *Ecology and Evolution* **11**: 10834–10867.

Hakkenberg CR, Goetz SJ. **2021**. Climate mediates the relationship between plant biodiversity and forest structure across the United States. *Global Ecology and Biogeography* **30**: 2245–2258.

Hakkenberg CR, Zhu K, Peet RK, Song C. **2018**. Mapping multi-scale vascular plant richness in a forest landscape with integrated LiDAR and hyperspectral remote-sensing. *Ecology* **99**: 474–487.

Hijmans R, Phillips S, Leathwick J, Elith J. 2023. dismo: Species Distribution Modeling. [WWW document] URL https://github.com/rspatial/dismo [accessed 24 August 2023].

Huang L, Koubek T, Weiser M, Herben T. **2018**. Environmental drivers and phylogenetic constraints of growth phenologies across a large set of herbaceous species. *Journal of Ecology* **106**: 1621–1633.

Husson F, Josse J, Le S, Mazet J. 2023. FactoMineR: Multivariate Exploratory Data Analysis and Data Mining. [WWW document] URL https://github.com/husson/FactoMineR [accessed 24 August 2023].

Hwang T, Song C, Vose JM, Band LE. **2011**. Topography-mediated controls on local vegetation phenology estimated from MODIS vegetation index. *Landscape Ecology* **26**: 541–556.

Jucker T, Hardwick SR, Both S, Elias DMO, Ewers RM, Milodowski DT, Swinfield T, Coomes DA. **2018**. Canopy structure and topography jointly constrain the microclimate of human-modified tropical landscapes. *Global Change Biology* **24**: 5243–5258.

Klosterman S, Melaas E, Wang J, Martinez A, Frederick S, O'Keefe J, Orwig DA, Wang Z, Sun Q, Schaaf C, *et al.* 2018. Fine-scale perspectives on landscape phenology from unmanned aerial vehicle (UAV) photography. *Agricultural and Forest Meteorology* **248**: 397–407.

For Peer Review

Klosterman S, Richardson AD. **2017**. Observing spring and fall phenology in a deciduous forest with aerial drone imagery. *Sensors* **17**: 2852.

Kokaly RF, Skidmore AK. **2015**. Plant phenolics and absorption features in vegetation reflectance spectra near 1.66 μm. *Int J Appl Earth Obs Geoinformation* **43**: 55–83.

Larue EA, Hardiman BS, Elliott JM, Fei S. **2019**. Structural diversity as a predictor of ecosystem function. *Environmental Research Letters* **14**: 114011.

LaRue EA, Wagner FW, Fei S, Atkins JW, Fahey RT, Gough CM, Hardiman BS. **2020**. Compatibility of aerial and terrestrial LiDAR for quantifying forest structural diversity. *Remote Sensing* **12**: 1407.

Li D, Stucky BJ, Deck J, Baiser B, Guralnick RP. **2019**. The effect of urbanization on plant phenology depends on regional temperature. *Nature Ecology and Evolution* **3**: 1661–1667.

Liu Z guo, Li K, Cai Y li, Fang Y. **2011**. Correlations between leafing phenology and traits: Woody species of evergreen broad-leaved forests in subtropical China. *Polish Journal of Ecology* **59**: 463–473.

Liu Y, Li G, Wu X, Niklas KJ, Yang Z, Sun S. **2021**. Linkage between species traits and plant phenology in an alpine meadow. *Oecologia* **195**: 409–419.

Liu S, Yan Z, Wang Z, Serbin S, Visser M, Zeng Y, Ryu Y, Su Y, Guo Z, Song G, *et al.* 2023. Mapping foliar photosynthetic capacity in sub-tropical and tropical forests with UAS-based imaging spectroscopy: Scaling from leaf to canopy. *Remote Sensing of Environment* **293**: 113612.

Maeda EE, Nunes MH, Calders K, de Moura YM, Raumonen P, Tuomisto H, Verley P, Vincent G, Zuquim G, Camargo JL. **2022**. Shifts in structural diversity of Amazonian forest edges detected using terrestrial laser scanning. *Remote Sensing of Environment* **271**: 112895.

Marconi S, Weinstein BG, Zou S, Bohlman SA, Zare A, Singh A, Stewart D, Harmon I, Steinkraus A, White EP. **2022**. Continental-scale hyperspectral tree species classification in the United States National Ecological Observatory Network. *Remote Sensing of Environment* **282**: 113264.

Martin ME, Plourde LC, Ollinger S V., Smith ML, McNeil BE. **2008**. A generalizable

For Peer Review

method for remote sensing of canopy nitrogen across a wide range of forest ecosystems. *Remote Sensing of Environment* **112**: 3511–3519.

Mäyrä J, Keski-Saari S, Kivinen S, Tanhuanpää T, Hurskainen P, Kullberg P, Poikolainen L, Viinikka A, Tuominen S, Kumpula T, *et al.* 2021. Tree species classification from airborne hyperspectral and LiDAR data using 3D convolutional neural networks. *Remote Sensing of Environment* **256**: 112322.

McGill BJ, Enquist BJ, Weiher E, Westoby M. **2006**. Rebuilding community ecology from functional traits. *Trends in Ecology and Evolution* **21**: 178–185.

Melaas EK, Friedl MA, Richardson AD. **2016**. Multiscale modeling of spring phenology across Deciduous Forests in the Eastern United States. *Global Change Biology* **22**: 792–805.

Messier J, McGill BJ, Enquist BJ, Lechowicz MJ. **2017**. Trait variation and integration across scales: is the leaf economic spectrum present at local scales? *Ecography* **40**: 685–697.

Messier J, McGill BJ, Lechowicz MJ. **2010**. How do traits vary across ecological scales? A case for trait-based ecology. *Ecology Letters* **13**: 838–848.

Misra G, Buras A, Heurich M, Asam S, Menzel A. **2018**. LiDAR derived topography and forest stand characteristics largely explain the spatial variability observed in MODIS land surface phenology. *Remote Sensing of Environment* **218**: 231–244.

Moon M, Richardson AD, Friedl MA. **2021a**. Multiscale assessment of land surface phenology from harmonized Landsat 8 and Sentinel-2, PlanetScope, and PhenoCam imagery. *Remote Sensing of Environment* **266**: 112716.

Moon M, Seyednasrollah B, Richardson AD, Friedl MA. **2021b**. Using time series of MODIS land surface phenology to model temperature and photoperiod controls on spring greenup in North American deciduous forests. *Remote Sensing of Environment* **260**: 112466.

Naikoo MI, Dar MI, Raghib F, Jaleel H, Ahmad B, Raina A, Khan FA, Naushin F. **2019**. Role and regulation of plants phenolics in abiotic stress tolerance: An overview. *Plant Signaling Molecules*: 157–168.

NEON (National Ecological Observatory Network). 2023. Discrete return LiDAR point cloud (DP1.30003.001). https://doi.org/10.48443/xxby-5a18.

Niinemets Ü, Valladares F. **2004**. Photosynthetic acclimation to simultaneous and

For Peer Review

interacting environmental stresses along natural light gradients: Optimality and constraints. *Plant Biology* **6**: 254–268.

Noda HM, Muraoka H, Nasahara KN, Saigusa N, Murayama S, Koizumi H. **2015**. Phenology of leaf morphological, photosynthetic, and nitrogen use characteristics of canopy trees in a cool-temperate deciduous broadleaf forest at Takayama, central Japan. *Ecological Research* **30**: 247–266.

Osada N. **2017**. Relationships between the timing of budburst, plant traits, and distribution of 24 coexisting woody species in a warm-temperate forest in Japan. *American Journal of Botany* **104**: 550–558.

Osada N, Hiura T. **2019**. Intraspecific differences in spring leaf phenology in relation to tree size in temperate deciduous trees. *Tree Physiology* **39**: 782–791.

Pau S, Wolkovich EM, Cook BI, Davies TJ, Kraft NJB, Bolmgren K, Betancourt JL, Cleland EE. **2011**. Predicting phenology by integrating ecology, evolution and climate science. *Global Change Biology* **17**: 3633–3643.

Peng J, Albergel C, Balenzano A, Brocca L, Cartus O, Cosh MH, Crow WT, Dabrowska-Zielinska K, Dadson S, Davidson MWJ, *et al.* 2021. A roadmap for high-resolution satellite soil moisture applications – confronting product characteristics with user requirements. *Remote Sensing of Environment* **252**: 112162.

Planet, 2022. Planet Imagery Product Specification [WWW Document] URL https://assets.planet.com/docs/Planet_Combined_Imagery_Product_ Specs_letter_screen.pdf [accessed 24 August 2023].

Polgar CA, Primack RB. **2011**. Leaf-out phenology of temperate woody plants: From trees to ecosystems. *New Phytologist* **191**: 926–941.

Poorter H, Poorter H, Niinemets Ü, Poorter L, Wright IJ, Villar R. **2009**. Causes and consequences of variation in leaf mass per area (LMA): a meta-analysis. *New phytologist* **182**: 565–588.

R Core Team. 2023. R: a language and environment for statistical computing. Vienna, Austria: R Foundation for Statistical Computing. [WWWdocument] URL https://www.R-project.org/ [accessed 24 August 2021].

Reich PB, Walters MB, Ellsworth DS. **1997**. From tropics to tundra: Global convergence in

For Peer Review

plant functioning. *Proceedings of the National Academy of Sciences of the United States of America* **94**: 13730–13734.

Ribeiro C, Stitt M, Hotta CT. **2022**. How Stress Affects Your Budget—Stress Impacts on Starch Metabolism. *Frontiers in Plant Science* **13**: 774060.

Roussel JR, Auty D, Coops NC, Tompalski P, Goodbody TRH, Meador AS, Bourdon JF, de Boissieu F, Achim A. **2020**. lidR: An R package for analysis of Airborne Laser Scanning (ALS) data. *Remote Sensing of Environment* **251**: 112061.

Seiwa K. **1999**. Changes in leaf phenology are dependent on tree height in Acer mono, a deciduous broad-leaved tree. *Annals of Botany* **83**: 355–361.

Shen M, Wang S, Jiang N, Sun J, Cao R, Ling X, Fang B, Zhang L, Zhang L, Xu X, *et al.* 2022. Plant phenology changes and drivers on the Qinghai–Tibetan Plateau. *Nature Reviews Earth and Environment* **3**: 633–651.

de Souza ACP, da Costa RC. **2020**. Differences in leaf phenology between juvenile and adult individuals of two tree species in a seasonally dry tropical woodland. *Austral Ecology* **45**: 240–248.

Sporbert M, Jakubka D, Bucher SF, Hensen I, Freiberg M, Heubach K, König A, Nordt B, Plos C, Blinova I, *et al.* 2022. Functional traits influence patterns in vegetative and reproductive plant phenology - a multi-botanical garden study. *New Phytologist* **235**: 2199–2210.

Stark S, Väisänen M, Ylänne H, Julkunen-Tiitto R, Martz F. **2015**. Decreased phenolic defence in dwarf birch (Betula nana) after warming in subarctic tundra. *Polar Biology* **38**: 1993–2005.

Sun S, Jin D, Li R. **2006**. Leaf emergence in relation to leaf traits in temperate woody species in East-Chinese Quercus fabri forests. *Acta Oecologica* **30**: 212–222.

Toda M, Richardson AD. **2018**. Agricultural and Forest Meteorology Estimation of plant area index and phenological transition dates from digital repeat photography and radiometric approaches in a hardwood forest in the Northeastern United States. *Agricultural and Forest Meteorology* **249**: 457–466.

Wang Z, Chlus A, Geygan R, Ye Z, Zheng T, Singh A, Couture JJ, Cavender-Bares J, Kruger EL, Townsend PA. **2020**. Foliar functional traits from imaging spectroscopy across

For Peer Review

biomes in eastern North America. *New Phytologist* **228**: 494–511.

Wang Z, Townsend PA, Kruger EL. **2022**. Leaf spectroscopy reveals divergent inter- and intra-species foliar trait covariation and trait–environment relationships across NEON domains. *New Phytologist* **235**: 923–938.

Wang Z, Townsend PA, Schweiger AK, Couture JJ, Singh A, Hobbie SE, Cavender-Bares J. **2019**. Mapping foliar functional traits and their uncertainties across three years in a grassland experiment. *Remote Sensing of Environment* **221**: 405–416.

Wang X, Wu C, Liu Y, Peñuelas J, Peng J. **2023**. Earlier leaf senescence dates are constrained by soil moisture. *Global Change Biology* **29**: 1557–1573.

Wang J, Zhang X, Rodman K. **2021**. Land cover composition , climate , and topography drive land surface phenology in a recently burned landscape : An application of machine learning in phenological modeling. *Agricultural and Forest Meteorology* **304**–**305**: 108432.

Wolkovich EM, Cook BI, Davies TJ. **2014**. Progress towards an interdisciplinary science of plant phenology: Building predictions across space, time and species diversity. *New Phytologist* **201**: 1156–1162.

Wright IJ, Reich PB, Westoby M, Ackerly DD, Baruch Z, Bongers F, Cavender-Bares J, Chapin T, Cornellssen JHC, Diemer M, *et al.* 2004. The worldwide leaf economics spectrum. *Nature* **428**: 821–827.

Wu S, Wang J, Yan Z, Song G, Chen Y, Ma Q, Deng M, Wu Y, Zhao Y, Guo Z, *et al.* 2021. Monitoring tree-crown scale autumn leaf phenology in a temperate forest with an integration of PlanetScope and drone remote sensing observations. *ISPRS Journal of Photogrammetry and Remote Sensing* **171**: 36–48.

Xia J, Niu S, Ciais P, Janssens IA, Chen J, Ammann C, Arain A, Blanken PD, Cescatti A, Bonal D, *et al.* 2015. Joint control of terrestrial gross primary productivity by plant phenology and physiology. *Proceedings of the National Academy of Sciences of the United States of America* **112**: 2788–2793.

Xie Y, Civco DL, Silander JA. **2018**. Species-specific spring and autumn leaf phenology captured by time-lapse digital cameras. *Ecosphere* **9**: e02089.

Xu Z, Shen X, Cao L, Coops NC, Goodbody TRH, Zhong T, Zhao W, Sun Q, Ba S, Zhang Z, *et al.* 2020. Tree species classification using UAS-based digital aerial

For Peer Review

photogrammetry point clouds and multispectral imageries in subtropical natural forests. *Int J Appl Earth Obs Geoinformation* **92**: 102173.

Yan Z, Sardans J, Peñuelas J, Detto M, Smith NG, Wang H, Guo L, Hughes AC, Guo Z, Lee CKF, *et al.* 2023. Global patterns and drivers of leaf photosynthetic capacity: The relative importance of environmental factors and evolutionary history. *Global Ecology and Biogeography* **32**: 668–682.

Yang J, Medlyn BE, Barton CVM, Churchill AC, De Kauwe MG, Jiang M, Krishnananthaselvan A, Tissue DT, Pendall E, Power SA. 2023. Green-up and brown-down: Modelling grassland foliage phenology responses to soil moisture availability. *Agricultural and Forest Meteorology* **328**: 109252.

Yin J, Fridley JD, Smith MS, Bauerle TL. 2016. Xylem vessel traits predict the leaf phenology of native and non-native understorey species of temperate deciduous forests. *Functional Ecology* **30**: 206–214.

Yin XH, Sterck F, Hao GY. 2018. Divergent hydraulic strategies to cope with freezing in co-occurring temperate tree species with special reference to root and stem pressure generation. *New Phytologist* **219**: 530–541.

Zeng L, Wardlow BD, Xiang D, Hu S, Li D. 2020. A review of vegetation phenological metrics extraction using time-series, multispectral satellite data. *Remote Sensing of Environment* **237**: 111511.

Zhao Y, Lee CKF, Wang Z, Wang J, Gu Y, Xie J, Law YK, Song G, Bonebrake TC, Yang X, *et al.* 2022. Evaluating fine-scale phenology from PlanetScope satellites with ground observations across temperate forests in eastern North America. *Remote Sensing of Environment* **283**: 113310.

For Peer Review